Received: 2 April 2020 | Accepted: 25 April 2020

DOI: 10.1002/ardp.202000106

FULL PAPER

DPhG ARCH PHARM Archiv der Pharmazie

Racemic total synthesis and evaluation of the biological activities of the isoquinoline–benzylisoquinoline alkaloid muraricine

Ramona Schütz | Martin Müller | Susanne Gerndt | Karin Bartel | Franz Bracher

Department of Pharmacy, Center for Drug Research, Ludwig-Maximilians-University of Munich, Munich, Germany

Correspondence
Franz Bracher, Department of Pharmacy, Center for Drug Research, Ludwig-Maximilians-University of Munich, Butenandtstr. 5–13, 81377 Munich, Germany.
Email: franz.bracher@cup.uni-muenchen.de

Funding information
Deutsche Forschungsgemeinschaft, Grant/Award Number: Project BR1034/7-1

Abstract

The first racemic total synthesis of the isoquinoline–benzylisoquinoline alkaloid muraricine is reported herein. Pharmacological characterization identified muraricine as a moderate inhibitor of P-glycoprotein, a crucial factor of multidrug resistance in cancer. When combined with vincristine, muraricine partly reversed the chemoresistance of vincristine-resistant leukemia cells at a nontoxic concentration. Furthermore, no cytotoxic effects on noncancerous human cells in therapeutically relevant concentrations were observed.

KEYWORDS

isoquinoline–benzylisoquinoline alkaloid, multidrug resistance, muraricine, P-gp inhibition

1 | INTRODUCTION

Bisbenzylisoquinolines are a large and structurally diverse subclass of the widely distributed benzylisoquinoline alkaloids.[1–3] In this chemotype, typically two tetrahydroisoquinoline units are connected by two (or more) diaryl ether (in some cases also biaryl) units to result in rigid, macrocyclic compounds, as exemplified by the structure of tetrandrine (**1**).[4] Numerous biological activities have been described for bisbenzylisoquinoline and several monomeric benzylisoquinoline alkaloids including anticancer,[5–9] multidrug resistance reversing,[10–15] antiviral,[16,17] antimicrobial,[18] and calcium channel-blocking activities.[19,20] Moreover, *seco*-analogues (so-called *seco*-bisbenzylisoquinoline alkaloids) have been detected, mainly in plants from the families Berberidaceae and Annonaceae.[21] There is some evidence that these *seco*-bisbenzylisoquinolines of natural origin are formed by oxidative degradation or by chemical and enzymatic cleavage[22] of parent bisbenzylisoquinoline alkaloids, probably as a first step of alkaloid catabolism in plant cells.[23] A couple of artefacts identical to these alkaloids were obtained by controlled photooxidation of bisbenzylisoquinoline alkaloids.[24,25]

In these *seco*-compounds, one or more bonds of the macrocyclic bisbenzylisoquinoline core are formally broken, with the most typical first scission between C-1 of an isoquinoline ring and the adjacent benzylic methylene group, as shown for *seco*-isotetrandrine (**2**).[26] But there are also examples for formal cleavage of a diaryl ether bridge between two isoquinoline units, as shown for berbamunine (**3**).[27] The tetrahydroisoquinolin-1-one unit of *seco*-bisbenzylisoquinolines (e.g., **2**) can formally be reduced to a tetrahydroisoquinoline, as shown for chenabine (**4**), but the mechanism of the biosynthesis is still unclear.[28] In certain cases, parts of the molecules are lost, as demonstrated for bargustanine (**5**),[29] where a complete benzyl unit is missing, and small "dimeric" isoquinolone alkaloids like berbidine (**6**),[23,30] in which both benzyl residues were cleaved off (Figure 1).

Recently, a novel *seco*-bisbenzylisoquinoline alkaloid, muraricine (**7**), was isolated from *Berberis vulgaris* (Berberidaceae) by Hostalkova et al.[31] Based on the analogy with related alkaloids, (*R*) configuration was postulated for **7**. In this alkaloid, similar to bargustanine (**5**), a diaryl ether bridge connecting two isoquinoline units is still present, and formally one benzyl unit is lost. This compound showed moderate butyrylcholinesterase inhibition during initial investigations.[31] This prompted us to develop a first total synthesis of racemic muraricine (*rac*-**7**) for providing sufficient amounts for further pharmacological characterization.

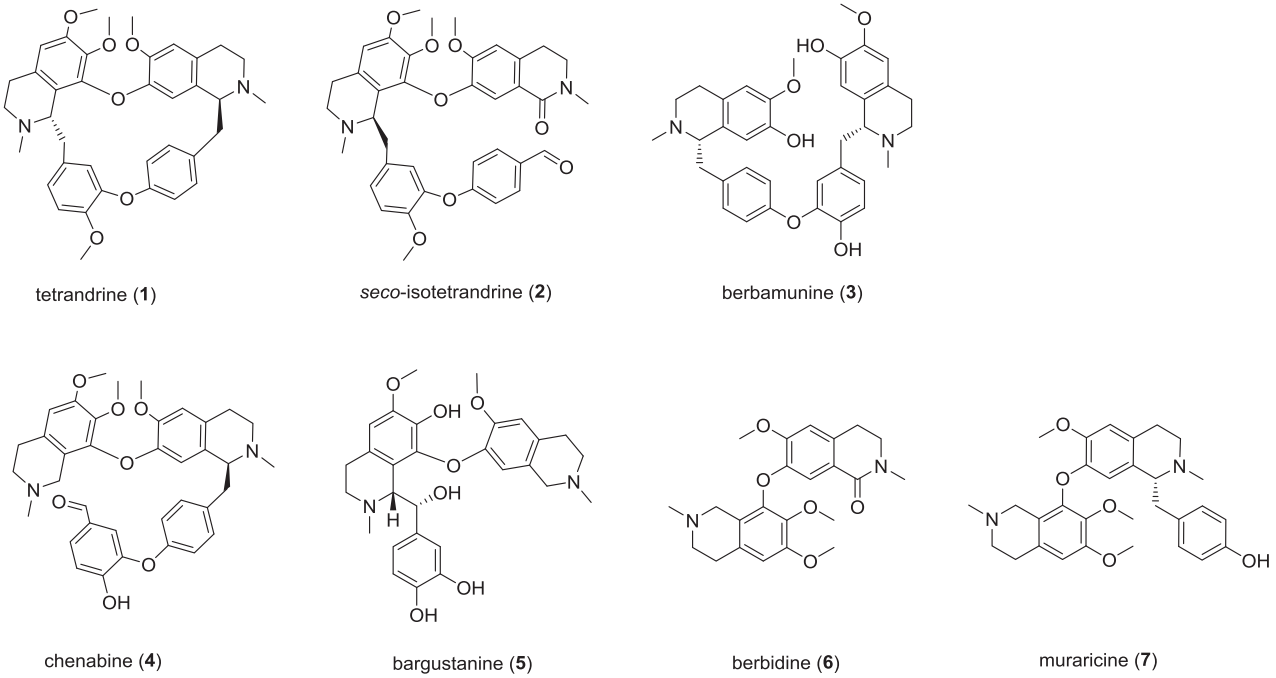

FIGURE 1 Bisbenzylisoquinoline alkaloids and naturally occurring *seco*-analogues

Based on our recently published racemic synthesis of the bisbenzylisoquinoline alkaloids tetrandrine (**1**) and isotetrandrine,[32] we herein present the first total synthesis of racemic muraricine (*rac*-**7**). Key steps of this approach are *N*-acyl Pictet–Spengler condensations for the formation of the tetrahydroisoquinoline moieties and a copper-catalyzed Ullmann coupling for the construction of the diaryl ether bridge.

Focus of the pharmacological evaluation of muraricine (*rac*-**7**) is the antiproliferative effect against several cancer cell lines, the evaluation of toxicity to noncancerous cells, chemoresistance reversing property by inhibition of the P-glycoprotein (P-gp), calcium channel-blocking activities, and antimicrobial effects.

2 | RESULTS AND DISCUSSION

2.1 | Chemistry

The total synthesis of racemic muraricine (*rac*-**7**) requires the construction of an *N*-methylated 1-benzyltetrahydroisoquinoline subunit, which is connected via a diaryl ether bridge with a 1-unsubstituted *N*-methylated tetrahydroisoquinoline. Very recently, we reported on a new modular total racemic synthesis[32] of tetrandrine (**1**) and isotetrandrine, for which we optimized both the diaryl ether synthesis (Ullmann coupling) and the construction of *N*-methylated 1-benzyltetrahydroisoquinolines using methoxystyrenes as arylacetaldehyde equivalents in *N*-acyl Pictet–Spengler condensations. Conveniently, one intermediate of this (iso)tetrandrine synthesis (**8**; compound no. 19 in Ref. [32]) lends itself to be used as a precursor of racemic muraricine (*rac*-**7**). Compound **8** is readily available in high-yielding steps starting from two commercially available substituted benzaldehydes (4-(benzyloxy)benzaldehyde, 3-bromo-4,5-dimethoxybenzaldehyde) and one arylethylamine (vanillin-derived 4-hydroxy-3-methoxyphenethylamine). A detailed scheme on the preparation of intermediate **8** is presented in the Supporting Information Data.

Trifluoroacetic acid-mediated *N*-acyl Pictet–Spengler reaction of racemic **8** with paraformaldehyde in dichloromethane gave a mixture of the ethoxycarbonyl-protected tetrahydroisoquinoline **9a** and a side product with an identical mass. Most likely, the minor component is the regioisomer, **9b**, resulting from two possible directions of cyclization of the 3,4,5-trisubstituted arylethylamine derivative **8** (Scheme 1). The ratio of the products **9a**:**9b** is 69:31, as determined by high-performance liquid chromatography (HPLC). The formation of regioisomers in electrophilic cyclizations such as Pictet–Spengler reactions is a known problem, which in certain cases can be controlled by solvent-directed approaches.[33,34] When conducting *N*-acyl Pictet–Spengler condensation in polar solvents such as trifluoroethanol or methanol following Kayhan's protocol,[34] the reaction unfortunately proceeded notably slower and was incomplete. From the obtained mixture, the desired isomer **9a** was isolated in good yield (68%) readily by flash column chromatography (FCC). This regioisomer **9a** could be unambiguously identified by 2D nuclear magnetic resonance (NMR) experiments (heteronuclear multiple bond correlation [HMBC] of **9a** and by nuclear Overhauser effect spectroscopy [NOESY] experiments of *rac*-**7**, respectively). Finally, bis-carbamate **9a** was converted to racemic muraricine (*rac*-**7**) in 23% yield by simultaneous reduction of both ethoxycarbonyl groups to *N*-methyl groups using lithium alanate (Scheme 1). The NMR data of product *rac*-**7** were in full agreement with the data

SCHEME 1 Total synthesis of racemic muraricine (*rac*-**7**). DCM, dichloromethane; rt, room temperature; TFA, trifluoroacetic acid; THF, tetrahydrofuran

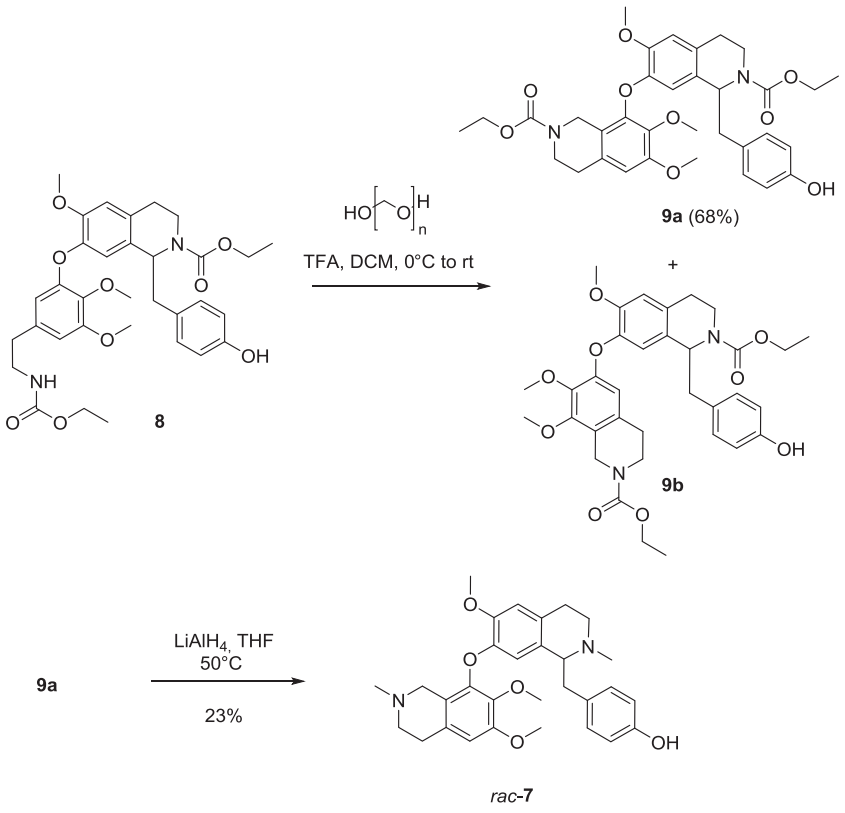

published for the natural alkaloid **7**.[31] The proposed structure of isolated muraricine (**7**) has herewith been confirmed.

2.2 | Pharmacology

As already mentioned, the only reported biological activity of muraricine (**7**) is a moderate butyrylcholinesterase inhibition.[31] As various biological activities have been described for the class of bisbenzylisoquinoline and benzylisoquinoline alkaloids as discussed above, we submitted synthetic *rac*-**7** to our screening systems for antiproliferative/cytotoxic, chemoresistance reversing, and antimicrobial and calcium channel-modulating activities.

2.2.1 | Antiproliferative activity

Antiproliferative effects of *rac*-**7** were investigated against hepatocellular carcinoma (HepG2), colorectal adenocarcinoma (HCT-15), and bladder carcinoma (T24) cell lines and determined by CellTiter-Blue® assay. The bisbenzylisoquinoline alkaloid tetrandrine (**1**) was used as a reference compound, whereas tetrandrine (**1**) showed significant activity against the three tumor cell lines; the truncated analogue *rac*-**7** did only show very low antiproliferative effects and no cytotoxic activity (Figure 2). These findings add to results of a structure–activity relationship study by Kupchan and Altland.[9] In this investigation, both macrocyclic bisbenzylisoquinolines and *seco*-analogues which retained a

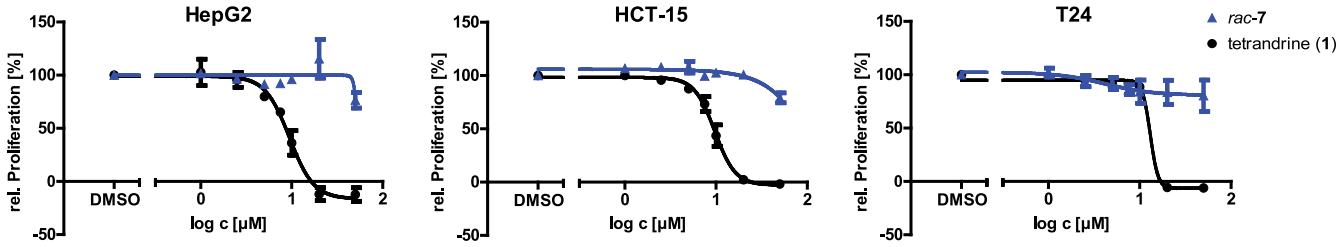

FIGURE 2 Antiproliferative effects of *rac*-**7** on hepatocellular carcinoma (HepG2), colorectal adenocarcinoma (HCT-15) and bladder carcinoma (T24) cell lines were determined by CellTiter-Blue® assay. Cells were incubated with the respective concentrations for 72 hr and proliferation is shown as percentage of vehicle control after subtraction of the zero value. Tetrandrine (**1**) served as control. Line graphs display mean ± *SEM* of three independent experiments. DMSO, dimethyl sulfoxide; *SEM*, standard error of the mean

diaryl ether bridge connecting both benzyl groups showed antiproliferative/cytotoxic effects, whereas trivial monomeric benzyltetrahydroisoquinolines were virtually inactive.

2.2.2 | Toxicity

As tetrandrine (**1**) and other bisbenzylisoquinoline alkaloids are also known to cause severe toxicity in liver[35–38] and lungs, [39–41] we investigated whether *rac*-**7** is toxic to noncancerous cells. For that purpose, human umbilical vein endothelial cells (HUVECs) were treated with 10, 20, and 50 µM for 6 hr and cell viability was assessed by quantifying the intracellular adenosine triphosphate (ATP) content. As expected, tetrandrine (**1**) strongly and dose-dependently affected the viability of HUVECs. In contrast, no significant toxicity to endothelial cells was observed upon *rac*-**7** treatment (Figure 3).

2.2.3 | Inhibition of P-gp

As pointed out, *rac*-**7** does not have direct antitumor effects. Hence, we aimed to evaluate its potential as an add-on in combination therapy. Natural alkaloids have been shown to improve the response to several antitumor drugs by targeting the P-gp.[10,11,42] P-gp facilitates the efflux of cytostatic drugs and thereby represents a major cause of treatment failure and resistance to common cancer therapeutics.[10] As no clinically approved treatment options targeting P-gp are available so far, there is a need for identifying novel, safe, and efficacious P-gp inhibitors. Inhibition of P-gp is mostly described for macrocyclic bisbenzylisoquinolines like tetrandrine (**1**)[42,43] and related alkaloids,[10] but also for some *seco*-analogues, such as dauricine and daurisoline.[44,45] Therefore, we investigated the influence of *rac*-**7** on the accumulation of the P-gp model substrate calcein-acetoxymethyl (AM) in vincristine-resistant

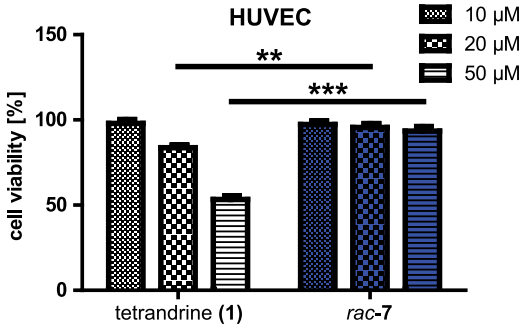

FIGURE 3 Acute toxicity to noncancerous human umbilical vein endothelial cells is shown. Cells were treated for 6 hr with *rac*-**7** and tetrandrine (**1**) (10, 20, 50 µM) for 6 hr. Cell viability was determined by quantifying the cellular adenosine triphosphate content applying a CellTiter-Glo® cell assay and is displayed as percentage of vehicle control as mean ± standard error of the mean of three independent experiments (one-way analysis of variance followed by Tukey's multiple comparison test; $^{**}p < .01$, $^{***}p < .001$)

CEM (VCR-R CEM) cells, leukemia cells that overexpress P-gp. We found a dose-dependent increase of calcein fluorescence (Figure 4a–c). Although the inhibition of P-gp-mediated calcein-AM efflux was weaker than that of the known inhibitor verapamil (Figure 4b,c), P-gp could be identified as a target of *rac*-**7** (Figure 4a,c). Verapamil was used as a positive control as the treatment did not affect cell viability under the chosen conditions. Consequently, P-gp inhibitory activity can be achieved by suitably decorated open-chain mimetics (*seco*-analogues) of complex, macrocyclic bisbenzylisoquinolines. To test if a combination of VCR with *rac*-**7** provides a therapeutic benefit, apoptosis of VCR-R CEM cells was evaluated. For both tested concentrations of VCR (0.1 and 1 µM), significantly increased apoptosis rates were detected when it was combined with nontoxic concentrations of *rac*-**7** (25 µM; Figure 4d). Taken together, these results demonstrate that *rac*-**7** represents a nontoxic *seco*-analogue of tetrandrine (**1**) with the potential to overcome drug resistance in cancer. P-gp-mediated drug efflux is not only implicated in tumor therapy but also represents a hurdle for the treatment of other diseases such as HIV and bacterial infections.[11] Eradication of HIV reservoirs in the central nervous system, for instance, is partly prevented by efflux transporters at the blood–brain barrier, including P-gp.[46] Consequently, this study provides the basis for further investigating the potential of *rac*-**7** to overcome resistance mechanisms by the efflux transporter P-gp.

2.2.4 | Calcium imaging

To determine whether *rac*-**7** is an inhibitor of the calcium channel, two-pore channel 2 (TPC2), Ca^{2+}-imaging experiments were performed using the recently published TPC2 activator TPC2-A1-N.[47] The response of TPC2-A1-N in HEK293 cells stably expressing $TPC2^{L11A/L12A}$ was not blocked by *rac*-**7** compared with a dimethyl sulfoxide (DMSO) control, whereas tetrandrine was able to block the activation (Figure 5a,b). Hence, *rac*-**7** does not show inhibitory activity on TPC2.

2.2.5 | Antimicrobial activity

We tested *rac*-**7** for antimicrobial activity in a standard agar diffusion assay against Gram-positive (*Streptococcus entericus*, *Staphylococcus equorum*) and Gram-negative bacteria (*Escherichia coli*, *Pseudomonas marginalis*), and against fungi (*Yarrowia lipolytica*, *Saccharomyces cerevisiae*). There was no zone of inhibition observed in any experiment; consequently, *rac*-**7** does not exhibit antimicrobial activity against the above-listed germs.

3 | CONCLUSION

In summary, we have developed the first total synthesis of racemic muraricine (*rac*-**7**) in a total of 10 steps. The overall yield amounts to

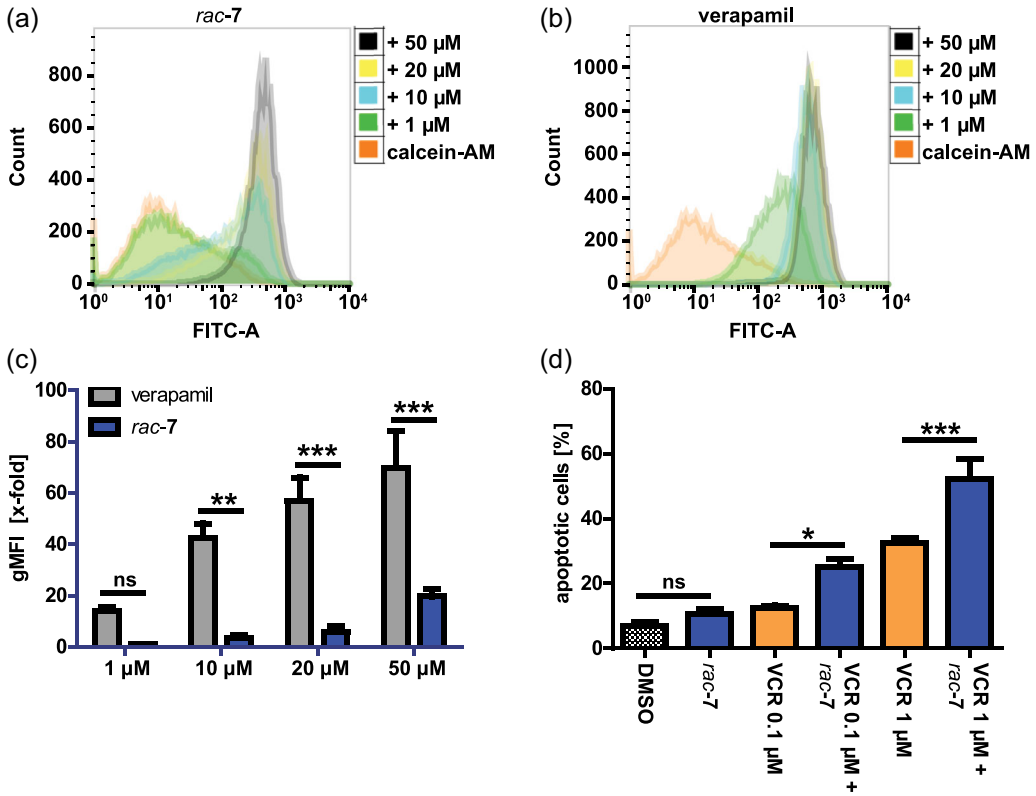

FIGURE 4 (a,b) Retention of the P-glycoprotein model substrate calcein-AM in vincristine-resistant CEM (VCR-R CEM) cells was determined by flow cytometry. Cells were incubated with calcein-AM, in the presence or absence of increasing concentrations of *rac*-**7** and the positive control verapamil (1, 10, 20, and 50 µM). Histograms of cell populations are shown. The experiment was performed in triplicate and one representative experiment is shown. (c) Quantification and statistical analysis of data from (a,b). Bar graph displays mean ± *SEM* of three independent experiments (one-way ANOVA followed by Tukey's multiple comparison test; $^{**}p < .01$, $^{***}p < .001$). (d) Percentage of apoptotic cells is shown. VCR-R CEM cells were treated with VCR (0.1 and 1 µM) with or without *rac*-**7** (25 µM) for 48 hr. Apoptotic cells were quantified by propidium iodide staining and flow cytometry. Bar graph displays mean ± *SEM* of three independent experiments (one-way ANOVA followed by Tukey's multiple comparison test; $^{*}p < .05$, $^{***}p < .001$). AM, acetoxymethyl; ANOVA, analysis of variance; DMSO, dimethyl sulfoxide; FITC, fluorescein isothiocyanate; ns, not significant; *SEM*, standard error of the mean

3.8% along the longest sequence. We further investigated biological activities of this natural product and hereby focused on targets that are already known for the class of (bis)benzylisoquinoline alkaloids. Neither antiproliferative, antimicrobial, nor TPC2-blocking activity in Ca^{2+}-imaging experiments could be detected, whereas *rac*-muraricine could be identified as an inhibitor of P-gp, an important factor in the mechanism of multidrug resistance of tumors. Although the inhibitory effect of muraricine on this efflux pump is only moderate, significantly increased apoptosis rates were observed in combination with VCR. Hence, *rac*-muraricine was able to overcome drug resistance to a commonly used chemotherapeutic drug. Moreover, no acute cytotoxicity to healthy human cells (HUVEC) in concentrations higher than that required for reversing chemoresistance was detected for *rac*-muraricine. These findings suggest that muraricine may serve as a potential lead structure in the development of new nontoxic P-gp inhibitors. Based on our synthetic approach, systematic structure variations of muraricine can be part of future drug design projects as the clinical need of P-gp inhibitors for the treatment of chemoresistant tumors is high.

4 | EXPERIMENTAL

4.1 | Chemistry

4.1.1 | General

All solvents and reagents were purchased from commercial suppliers and were used without further purification, unless mentioned otherwise. Thin-layer chromatography was carried out on 0.2 mm silica gel polyester plates with a fluorescence indicator (POLYGRAM SIL G/UV254; Macherey-Nagel). NMR spectra were recorded with a 400-MHz (400 MHz for ^{1}H and 101 MHz for ^{13}C) or 600-MHz Bruker BioSpin Avance spectrometer (599 MHz for ^{1}H and 151 MHz for ^{13}C). Peak assignments were based on 2D NMR experiments using standard pulse programs (correlation spectroscopy [COSY], heteronuclear multiple quantum correlation/heteronuclear single quantum correlation [HSQC/HMQC], distortionless enhancement of polarization transfer [DEPT], HMBC, and NOESY). Chemical shifts were referenced to the residual solvent signal ($CDCl_3$: $\delta_H = 7.26$ ppm, $\delta_C = 77.16$ ppm). For the

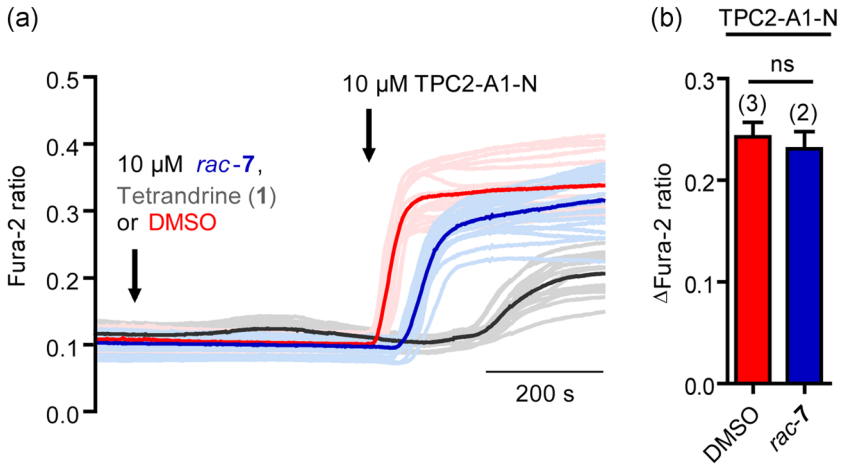

FIGURE 5 Ca^{2+}-imaging results of *rac*-**7**, tetrandrine (**1**), and a DMSO control using the TPC2 activator TPC2-A1-N. (a) Representative Ca^{2+} signals recorded from HEK293 cells stably expressing $TPC2^{L11A/L12A}$–RFP. After applying *rac*-**7** (10 µM; blue lines, $n = 19$ single cells), tetrandrine (**1**, 10 µM; gray lines, $n = 17$ single cells) or DMSO (0.1% in HBS; red lines, $n = 16$ single cells) and monitoring the signal for 400 s, cells were stimulated with TPC2-A1-N (10 µM) and further recorded for 400 s. Means are represented as highlighted lines, whereas single-cell traces of each experiment are in the background. (b) Statistical analysis of the maximal change in the Fura-2 ratio (mean ± *SEM*) with the number of independent experiments in parentheses. An unpaired *t*-test was applied. DMSO, dimethyl sulfoxide; HBS, HEPES-buffered solution; ns, not significant; RFP, red fluorescent protein

characterization of rotamers, a temperature program was employed for recording both 1D and 2D spectra. Hereby, chemical shifts were referenced to the signal of tetramethylsilane in deuterated tetrachloroethane (Tcl_2 [100°C]: $\delta_H = 5.92$ ppm, $\delta_C = 74.0$ ppm). Infrared (IR) spectra were recorded using a Jasco FT/IR-4100 (type A) instrument equipped with a diamond attenuated total reflection (ATR) unit (Jasco PRO450-S). High-resolution mass spectra (HRMS) were recorded using a Jeol MStation 700 or JMS-GCmate II Jeol instrument for electron impact ionization. Thermo Finnigan LTQ was used for electrospray ionization (ESI). HPLC purity was determined using Infinity Lab Poroshell 120EC-C18 and 120CN-C18 columns (2.7 µm, 100 × 3.0 mm), detected at 210 and 254 nm. Reaction monitoring by mass spectrometry was performed by atmospheric-pressure solids analysis probe via atmospheric-pressure chemical ionization on an Advion expression LC-MS device. Purification by FCC was performed using Merck Silica gel 60 (0.040–0.063 mm, 230–400 mesh ASTM). For quantitative analysis of compounds **9a**/**9b**, as well as for determination of the purity of all compounds, HPLC was performed on an Agilent Zorbax Eclipse Plus C18 column (5.0 µm, 150 × 4.6 mm) using the following methods: an eluent system as indicated below; flow 0.8 ml/min; temperature 50°C; Agilent 1100/1200 diode array detector ($\lambda = 210$ nm).

The InChI codes of compounds **9a** and *rac*-**7** together with some biological activity data are provided as Supporting Information Data.

4.1.2 | Synthesis of *N,N′*-bisnor-muraricine bis(ethylcarbamate) (9a)

Intermediate **8** (53.0 mg, 0.0871 mmol) was dissolved in 1.5 ml dichloromethane, and paraformaldehyde (5.2 mg, 0.174 mmol, 2.0 eq) was added. The mixture was cooled to 0°C, and trifluoroacetic acid (65 µl, 0.871 mmol, 10.0 eq) was slowly added. The reaction mixture was allowed to warm up to ambient temperature and stirred for 2 hr. Then, 1.0 ml of a saturated $NaHCO_3$ solution was added for neutralization and the mixture was extracted with dichloromethane (3 × 10 ml). The combined organic phases were dried over anhydrous Na_2SO_4 and concentrated in vacuo. Purification by FCC (20% ethyl acetate in dichloromethane, $R_f = 0.14$) gave the title compound as a white solid (36.8 mg, 0.0593 mmol, 68%). Mp: 91.0–93.0°C. ^{1}H NMR, COSY (400 MHz, Tcl_2, 100°C) δ [ppm] = 6.80–6.75 (m, 2H, 10-H, 14-H), 6.68 (s, 1H, 5-H), 6.61–6.57 (m, 2H, 11-H, 13-H), 6.51 (s, 1H, 5′-H), 6.03 (s, 1H, 8-H), 4.95 (t, $J = 6.6$ Hz, 1H, 1-H), 4.41 (d, $J = 17.1$ Hz, 1H, 1′-H), 4.29 (d, $J = 17.1$ Hz, 1H, 1′-H), 4.13 (q, $J = 7.1$ Hz, 2H, $'OCH_2CH_3$), 4.04 (q, $J = 7.1$ Hz, 2H, OCH_2CH_3), 3.87 (s, 3H, 6-OCH_3), 3.88–3.82 (m, 1H, 3-H), 3.82 (s, 3H, 6′-OCH_3), 3.62–3.57 (m, 1H, 3′-H), 3.59 (s, 3H, 7′-OCH_3), 3.34–3.25 (m, 1H, 3-H), 2.91 (dd, $J = 13.6$, 6.0 Hz, 1H, α-H), 2.79–2.72 (m, 4H, α-H, 4′-H, 4-H), 2.61 (dt, $J = 16.0$, 5.2 Hz, 1H, 4-H), 1.23 (t, $J = 7.1$ Hz, 3H, 2′-$NCOOCH_2CH_3$), 1.17 (t, $J = 7.1$ Hz, 3H, 2-$NCOOCH_2CH_3$). ^{13}C NMR, HSQC, HMBC (101 MHz, Tcl_2, 100°C) δ [ppm] = 156.0 (′*C*═O), 155.5 (*C*═O), 154.4 (C-12), 152.4 (C-6′), 148.5 (C-6), 146.2 (C-7), 145.9 (C-8′), 140.6 (C-7′), 130.6 (C-10, C-14), 130.4 (C-9), 130.2 (C-4a′), 129.3 (C-8a), 128.6 (C-4a), 120.2 (C-8a′), 115.4 (C-11, C-13), 114.9 (C-8), 113.9 (C-5), 109.8 (C-5′), 61.4 ($'OCH_2CH_3$), 61.2 (OCH_2CH_3), 60.7 (7′-OCH_3), 56.9 (6-OCH_3), 56.6 (6′-OCH_3), 56.3 (C-1), 42.3 (C-α), 41.5 (C-1′ and C-3′), 39.1 (C-3), 28.9 (C-4′), 28.2 (C-4), 14.70 (2′-$NCOOCH_2CH_3$), 14.66 (2-$NCOOCH_2CH_3$). IR (ATR): $\tilde{\nu}$ [cm^{-1}] = 2,925, 2,855, 1,670, 1,612, 1,513, 1,425, 1,236, 1,108, 1,023, 823, 769. Purity (HPLC) = 76% ($\lambda = 210$ nm) (70% acetonitrile, 30% water). HRMS (ESI): *m/z* calcd for $[C_{34}H_{40}N_2O_9 + H]^+$ 621.2807, found: 621.2806.

4.1.3 | Synthesis of racemic muraricine (*rac*-7)

Lithium alanate (25.7 mg, 0.677 mmol, 12.0 eq) was suspended in 1.0 ml anhydrous tetrahydrofuran (THF) under nitrogen atmosphere. A solution of **9a** (35.0 mg, 0.0564 mmol) in anhydrous THF was added dropwise and the resulting mixture was heated to 50°C for 3 hr. The reaction mixture was cooled to 0°C and slowly quenched with water. After alkalizing with a saturated $NaHCO_3$ solution, the mixture was extracted with ethyl acetate (3 × 10 ml). The combined organic phases were dried over anhydrous Na_2SO_4 and concentrated in vacuo. Purification by FCC (10% methanol and 2% triethylamine in ethyl acetate, R_f = 0.22) gave the title compound as a beige solid (8.0 mg, 0.0158 mmol, 23%). Mp: 63.0–65.0°C (Ref. [31]: no melting point given). ^{1}H NMR, COSY, NOESY (400 MHz [600 MHz for NOESY], $CDCl_3$) δ [ppm] = 6.66 (s, 1H, 5-H), 6.60 (d, J = 8.0 Hz, 2H, 10-H, 14-H), 6.53 (d, J = 8.0 Hz, 2H, 11-H, 13-H), 6.47 (s, 1H, 5′-H), 4.83 (s, 1H, 8-H), 3.89 (s, 3H, 6-OCH_3), 3.80 (s, 3H, 6′-OCH_3), 3.83–3.76 (m, 1H, 1′-H), 3.58 (dd, J = 10.5, 3.0 Hz, 1H, 1-H), 3.39 (s, 3H, 7′-OCH_3), 3.41–3.31 (m, 3H, α-H, 3-H, 4′-H), 3.29–3.22 (m, 1H, 1′-H), 3.12 (dd, J = 11.0, 5.4 Hz, 1H, 3′-H), 3.03–2.93 (m, 2H, 3-H, 4-H), 2.87–2.75 (m, 1H, 4-H), 2.70 (d, J = 16.6 Hz, 1H, 4′-H), 2.62 (s, 3H, 2-NCH_3), 2.61 (s, 3H, 2′-NCH_3), 2.53 (t, J = 11.8 Hz, 1H, α-H), 2.47–2.38 (m, 1H, 3′-H). ^{13}C NMR, HSQC, HMBC (101 MHz, $CDCl_3$) δ [ppm] = 156.4 (C-12), 152.1 (C-6′), 147.6 (C-6), 144.2 (C-7), 144.1 (C-8′), 138.9 (C-7′), 130.9 (C-10, C-14), 129.7 (C-9), 129.0 (C-4a′), 126.1 (C-8a), 125.6 (C-4a), 118.8 (C-8a′), 118.3 (C-11, C-13), 115.1 (C-8), 111.9 (C-5), 108.2 (C-5′), 65.2 (C-1), 60.2 (7′-OCH_3), 56.2 (6-OCH_3), 56.1 (6′-OCH_3), 53.0 (C-1′), 52.4 (C-3′), 45.6 (2′-NCH_3), 45.5 (C-3), 41.8 (2-NCH_3), 39.6 (C-α), 28.2 (C-4′), 24.6 (C-4). IR (ATR): $\tilde{\nu}$ [cm^{-1}] = 2,925, 2,850, 1,611, 1,512, 1,453, 1,259, 1,118, 1,064, 834, 796. Purity (HPLC) ≥ 95% (λ = 210 nm) (80% MeOH, 20% water, buffer pH 9). HRMS (ESI): m/z calcd for $[C_{30}H_{36}N_2O_5 + H]^+$ 505.2697, found: 505.2697.

4.2 | Biological assays

4.2.1 | Cell lines and culture

HCT-15 cells were purchased from ATCC. T24 cells were obtained from Dr. B. Mayer (Surgical Clinic, Ludwig-Maximilians-University [LMU], Munich). VCR-R CEM cells were kindly provided by Prof. Maria Kavallaris (University of New South Wales, Australia). HepG2 cells were obtained from German Research Centre of Biological Material (DSMZ). HepG2 and T24 cells were cultivated with Dulbecco's modified Eagle's medium (DMEM; PAN Biotech), HCT-15 and VCR-R CEM cells were cultivated with RPMI-1640 (PAN Biotech), and were used supplemented with 10% fetal calf serum (FCS; PAA Laboratories GmbH). HUVECs were purchased from PromoCell and cultivated with Endothelial Cell Growth Medium Kit Enhanced (PELO Biotech) supplemented with 10% FCS (PAA Laboratories GmbH) and 1% penicillin/streptomycin/amphotericin B (all purchased from PAN Biotech). HUVECs were cultured for a maximum of six passages. All cells were cultured at 37°C with 5% CO_2 with constant humidity.

4.2.2 | Cell proliferation assays

Antiproliferative effects were assessed by CellTiter-Blue cell viability assay as described previously.[48] Cells were seeded at the following densities: HepG2: 5×10^3 cells/well, HCT-15: 3×10^3 cells/well, T24: 10×10^3 cells/well.

4.2.3 | Acute toxicity assay

HUVECs were seeded at a density of 10×10^3 cells/well of a 96-well plate and allowed to adhere overnight. On the following day, cells were treated with the indicated concentrations of the respective compounds for 6 hr. Cellular ATP content was quantified by CellTiter-Glo® cell viability assay (Promega) as indicated by the manufacturer. Luminescence at 560 nm was recorded with an Orion II Microplate Luminometer (Berthold Detection Systems).

4.2.4 | Calcein-AM retention assay

The protocol was adapted from Robey et al.[42] Briefly, VCR-R CEM cells were seeded at a density of 0.15×10^6 cells/well of a 12-well plate and incubated for 4 hr. Subsequently, calcein-AM (200 nM; Biomol) and the potential P-gp inhibitors were added and incubated for 30 min. After incubation, cells were centrifuged (400*g*, 5 min), washed with phosphate-buffered saline and resuspended in RPMI-1640 without phenol red (PAN Biotech) containing the respective concentration of the P-gp inhibitor. Following a 60-min incubation time, calcein fluorescence was analyzed by flow cytometry on a FACSCalibur™ (Becton Dickinson).

4.2.5 | Apoptosis assay

VCR-R CEM cells were seeded at a density of 0.125×10^6 cells/well of a 24-well plate and incubated for 4 hr. Treatment was performed with the indicated concentrations for 48 hr. Apoptosis was determined by propidium iodide staining as described before[49] on FACSCalibur.

4.2.6 | Ca^{2+} imaging

Single-cell Ca^{2+}-imaging experiments were performed using Fura-2 as previously described.[50] HEK293 cells stably expressing $TPC2^{L11A/L12A}$–RFP (generated according to Gerndt et al.[47]) were cultured at 37°C with 5% of CO_2 in DMEM (Thermo Fisher Scientific), supplemented with 10% fetal bovine serum, 100 U/ml penicillin, and 0.1 mg/ml streptomycin. Cells were plated onto poly-L-lysine (Sigma-Aldrich)-coated glass coverslips and grown for 2–3 days. For Ca^{2+}-imaging experiments, cells were loaded for 1 hr at room temperature with Fura-2 AM (4.0 μM) and 0.005% (v/v) pluronic acid (both from

Thermo Fisher Scientific) in HEPES-buffered solution (HBS) comprising 138 mM NaCl, 6 mM KCl, 2 mM $MgCl_2$, 2 mM $CaCl_2$, 10 mM HEPES, and 5.5 mM D-glucose (adjusted to pH 7.4 with NaOH). After loading, cells were washed with HBS and mounted in an imaging chamber. All recordings were performed in HBS. Ca^{2+} imaging was performed using a Leica DMi8 live cell microscope. Fura-2 was excited at 340/380 nm. Emitted fluorescence was captured using a 515-nm long-pass filter. Compounds were prediluted in DMSO and stored as 10 mM stock solutions at −20°C, not exceeding 3 months. Working solutions were prepared directly before using by dilution with HBS.

4.2.7 | Agar diffusion assay

The bacteria and fungi, purchased from DSMZ, were cultivated on an AC agar (Sigma-Aldrich). Six-millimeter paper discs, impregnated with 30 µg of the tested compound or reference drug (tetracyclin/clotrimazole; both as a 1% [m/V] stock solution in DMSO) were placed on the agar. The bacteria media were incubated for 24 hr at 32°C, the fungi media for 48 hr at 28°C and the diameter of the zone of inhibition (mm) was registered. Tests were performed in triplicate.

4.2.8 | Statistical analysis

The GraphPad Prism software was used for statistical analysis. For some experiments, results were normalized to controls as indicated.

ACKNOWLEDGMENTS

We thank Bernadette Grohs for technical assistance with cell culture and flow cytometry experiments, as well as Martina Stadler for performing the tests for antimicrobial activity. We thank Prof. Dr. Christian Grimm, LMU Munich, for giving us access to his calcium-imaging facilities. Financial support was provided for F. B. by the Deutsche Forschungsgemeinschaft (project BR1034/7-1).

CONFLICT OF INTERESTS

The authors declare that there are no conflicts of interests.

ORCID

Ramona Schütz http://orcid.org/0000-0003-1282-6662
Martin Müller http://orcid.org/0000-0003-4513-8671
Franz Bracher http://orcid.org/0000-0003-0009-8629

REFERENCES

[1] C. Weber, T. Opatz *The Alkaloids: Chemistry and Biology* (Ed: H.-J. Knölker), Academic Press, New York, NY **2019**, p. 181.
[2] M. Shamma, *The Isoquinoline Alkaloids: Chemistry and Pharmacology*, Vol. 25, Academic Press, New York, NY **1972**.
[3] P. L. Schiff, *J. Nat. Prod.* **1997**, *60*, 934.
[4] H. Kondo, K. Yano, *Liebigs Ann. Chem.* **1932**, *497*, 90.
[5] O. N. P. Nguyen, C. Grimm, L. S. Schneider, Y.-K. Chao, C. Atzberger, K. Bartel, A. Watermann, M. Ulrich, D. Mayr, C. Wahl-Schott, M. Biel, A. M. Vollmar, *Cancer Res.* **2017**, *77*, 1427.
[6] A. M. Al-Ghazzawi, *BMC Chem.* **2019**, *13*, 13.
[7] N. Bhagya, K. R. Chandrashekar, *Biomed. Pharmacother.* **2018**, *97*, 624.
[8] K. H. Kim, I. K. Lee, C. J. Piao, S. U. Choi, J. H. Lee, Y. S. Kim, K. R. Lee, *Biorg. Med. Chem. Lett.* **2010**, *20*, 4487.
[9] S. M. Kupchan, H. W. Altland, *J. Med. Chem.* **1973**, *16*, 913.
[10] P. Joshi, R. A. Vishwakarma, S. B. Bharate, *Eur. J. Med. Chem.* **2017**, *138*, 273.
[11] S. Dewanjee, T. Dua, N. Bhattacharjee, A. Das, M. Gangopadhyay, R. Khanra, S. Joardar, M. Riaz, V. Feo, M. Zia-Ul-Haq, *Molecules* **2017**, *22*, 871.
[12] Z.-X. Qing, J.-L. Huang, X.-Y. Yang, J.-H. Liu, H.-L. Cao, F. Xiang, P. Cheng, J.-G. Zeng, *Curr. Med. Chem.* **2018**, *25*, 5088.
[13] L.-W. Fu, Z. A. Deng, Q. C. Pan, W. Fan, *Anticancer Res.* **2001**, *21*, 2273.
[14] A. M. Hall, C. J. Chang, *J. Nat. Prod.* **1997**, *60*, 1193.
[15] F. Frappier, A. Jossang, J. Soudon, F. Calvo, P. Rasoanaivo, S. Ratsimamanga-Urverg, J. Saez, J. Schrevel, P. Grellier, *Antimicrob. Agents Chemother.* **1996**, *40*, 1476.
[16] Y. Sakurai, A. A. Kolokoltsov, C.-C. Chen, M. W. Tidwell, W. E. Bauta, N. Klugbauer, C. Grimm, C. Wahl-Schott, M. Biel, R. A. Davey, *Science* **2015**, *347*, 995.
[17] G. S. Gunaratne, Y. Yang, F. Li, T. F. Walseth, J. S. Marchant, *Cell Calcium* **2018**, *75*, 30.
[18] K. Iwasa, M. Moriyasu, Y. Tachibana, H.-S. Kim, Y. Wataya, W. Wiegrebe, K. F. Bastow, L. M. Cosentino, M. Kozuka, K.-H. Lee, *Biorg. Med. Chem.* **2001**, *9*, 2871.
[19] C.-Y. Kwan, F. Achike, *Acta Pharm. Sin.* **2016**, *23*, 1057.
[20] J. P. Felix, V. F. King, J. L. Shevell, M. L. Garcia, G. J. Kaczorowski, I. R. C. Bick, R. S. Slaughter, *Biochemistry* **1992**, *31*, 11793.
[21] S. F. Hussain, *Baqai J. Health Sci.* **2018**, *21*, 58.
[22] T. Kametani, K. Fukumoto, K. Kigasawa, K. Wakisaka, *Chem. Pharm. Bull.* **1971**, *19*, 714.
[23] S. F. Hussain, M. T. Siddiqui, M. Shamma, *J. Nat. Prod.* **1989**, *52*, 317.
[24] I. R. C. Bick, J. B. Bremner, L. Van Thuc, P. Wiriyachitra, *J. Nat. Prod.* **1986**, *49*, 373.
[25] I. R. C. Bick, J. B. Bremner, P. Wiriyachitra, *Tetrahedron Lett.* **1971**, *12*, 4795.
[26] G. Schmeda-Hirschmann, M. Dutra-Behrens, G. Habermehl, J. Jakupovic, *Phytochemistry* **1996**, *41*, 339.
[27] K. T. Buck *The Alkaloids: Chemistry and Pharmacology* (Ed: A. Brossi), Academic Press, New York, NY **1987**, p. 130.
[28] J. E. Leet, V. Elango, S. F. Hussain, M. Shamma, *Heterocycles* **1983**, *20*, 425.
[29] A. Karimov, M. Yusupov, R. Shakirov, *Chem. Nat. Compd.* **1993**, *29*, 35.
[30] R. Schütz, S. Schmidt, F. Bracher, *Tetrahedron* **2020**, *76*, 131150.
[31] A. Hostalkova, J. Marikova, L. Opletal, J. Korabecny, D. Hulcova, J. Kunes, L. Novakova, D. I. Perez, D. Jun, T. Kucera, V. Andrisano, T. Siatka, L. Cahlikova, *J. Nat. Prod.* **2019**, *82*, 239.
[32] R. Schütz, M. Meixner, I. Antes, F. Bracher, *Org. Biomol. Chem.* **2020**, *18*, 3047. https://doi.org/10.1039/D0OB00078G
[33] B. Horst, M. J. Wanner, S. I. Jørgensen, H. Hiemstra, J. H. van Maarseveen, *J. Org. Chem.* **2018**, *83*, 15110.
[34] J. Kayhan, M. J. Wanner, S. Ingemann, J. H. van Maarseveen, H. Hiemstra, *Eur. J. Org. Chem.* **2016**, *2016*, 3705.
[35] L. Tainlin, H. Tingyi, Z. Changqi, Y. Peipei, Z. Qiong, *Ecotoxicol. Environ. Saf.* **1982**, *6*, 528.
[36] F. Li, Y. Z. Dong, D. Zhang, X. M. Zhang, Z. J. Lin, B. Zhang, *PLOS One* **2019**, *14*, e0216948.
[37] X. M. Qi, L. L. Miao, Y. Cai, L. K. Gong, J. Ren, *Acta Pharmacol. Sin.* **2013**, *34*, 1229.
[38] C. Yan, Q. Xin-Ming, G. Li-Kun, L. Lin-Lin, C. Fang-Ping, X. Ying, W. Xiong-Fei, L. Xiang-Hong, R. Jin, *Toxicology* **2006**, *218*, 1.

[39] H. Jin, L. Li, D. Zhong, J. Liu, X. Chen, J. Zheng, *Chem. Res. Toxicol.* **2011**, *24*, 2142.
[40] Y. Tian, S. Shen, Y. Jiang, Q. Shen, S. Zeng, J. Zheng, *Arch. Toxicol.* **2016**, *90*, 1737.
[41] H. Jin, S. Shen, X. Chen, D. Zhong, J. Zheng, *Toxicol. Appl. Pharmacol.* **2012**, *261*, 248.
[42] R. W. Robey, S. Shukla, E. M. Finley, R. K. Oldham, D. Barnett, S. V. Ambudkar, T. Fojo, S. E. Bates, *Biochem. Pharmacol.* **2008**, *75*, 1302.
[43] R. J. Kelly, R. W. Robey, C. C. Chen, D. Draper, V. Luchenko, D. Barnett, R. K. Oldham, Z. Caluag, A. R. Frye, S. M. Steinberg, T. Fojo, S. E. Bates, *Oncologist* **2012**, *17*, 512.
[44] S. Chai, K. K. W. To, G. Lin, *Chin. Med.* **2010**, *5*, 26.
[45] F. Tian, Q. C. Pan, *Chin. J. Cancer* **1996**, *15*, 410.
[46] N. Agrawal, J. Rowe, J. Lan, Q. Yu, C. A. Hrycyna, J. Chmielewski, *J. Med. Chem.* **2020**, *63*, 2131.
[47] S. Gerndt, C.-C. Chen, Y.-K. Chao, Y. Yuan, S. Burgstaller, A. Scotto Rosato, E. Krogsaeter, N. Urban, K. Jacob, O. N. P. Nguyen, M. T. Miller, M. Keller, A. M. Vollmar, T. Gudermann, S. Zierler, J. Schredelseker, M. Schaefer, M. Biel, R. Malli, C. Wahl-Schott, F. Bracher, S. Patel, C. Grimm, *eLife* **2020**, *9*, e54712.
[48] K. Vögerl, N. Ong, J. Senger, D. Herp, K. Schmidtkunz, M. Marek, M. Müller, K. Bartel, T. B. Shaik, N. J. Porter, D. Robaa, D. W. Christianson, C. Romier, W. Sippl, M. Jung, F. Bracher, *J. Med. Chem.* **2019**, *62*, 1138.
[49] C. Riccardi, I. Nicoletti, *Nat. Protoc.* **2006**, *1*, 1458.
[50] C. Grimm, S. Hassan, C. Wahl-Schott, M. Biel, *J. Pharmacol. Exp. Ther.* **2012**, *342*, 236.

SUPPORTING INFORMATION

Additional supporting information may be found online in the Supporting Information section.

How to cite this article: Schütz R, Müller M, Gerndt S, Bartel K, Bracher F. Racemic total synthesis and evaluation of the biological activities of the isoquinoline–benzylisoquinoline alkaloid muraricine. *Arch Pharm*. 2020;353:e2000106. https://doi.org/10.1002/ardp.202000106